Processing of grain-size functionally gradient bioceramics for implant applications

K. MORSI*
Department of Mechanical Engineering, San Diego State University, 5500 Campanile Drive, San Diego, California 92182, USA
E-mail: kmorsi@mail.sdsu.edu

H. KESHAVAN
Department of Mechanical and Aerospace Engineering, University of Missouri, Columbia, MO 65211, USA

S. BAL
Department of Orthopedic Surgery, University of Missouri, Columbia, MO 65211, USA

This paper reports work on the processing of functionally gradient alumina bioceramics with a continuously decreasing grain size across the thickness, with the view of ultimately utilizing high-quality nano/ultrafine powders only at the surface of an implant to provide superior wear and mechanical properties. A model of disc geometry is used to examine the feasibility of producing this brand of materials. Wet processing/ball milling and sequential slip casting procedures were used to de-agglomerate alumina powders and deposit green layers of varying particle sizes from 50 to 250 nm. Both pressure-less sintering and hot pressing were evaluated as high temperature sintering/consolidation processes. The results indicate that pressure-less sintering may not be suitable. Hot pressing, however, achieved very promising results producing near fully dense product with a grain size that gradually changes across its thickness.

Introduction

Artificial joint replacement has advanced considerably over the past three decades. Over 300 000 total hip and knee replacements are performed annually in the United States to restore function of diseased and damaged articular tissue [1]. The combination of the cobalt–chrome femoral head and ultra high molecular weight polyethylene (UHMWPE) acetabular liner reflects the current standard of care in artificial hip replacement [2]. Despite predictable success for the 10–15 years following the implantation of an artificial hip, late aseptic loosening of the components is virtually inevitable. Clinical results very clearly show that UHMWPE wear debris is currently creating problems in the young and active patients. Eventually, these sequences of events lead to loosening and failure of the prosthesis, requiring major repeat surgery. Efforts to increase the longevity of artificial hip replacements have focused mainly on reducing the quantity of wear generated at the bearing surfaces of these implants. Improvements in the quality of the metal-on-UHMPE articulation have contributed to reduced wear, and alternative bearing surfaces such as ceramic-on-ceramic have demonstrated some of the lowest wear rates reported in the literature [3]. Clinical trials with total hips that have an alumina-on-alumina bearing are currently underway at the University of Missouri Hospital at Columbia. Ceramic bearings presently used in hip replacement are composed of micrometer-sized grains. Particulate wear generated from such bearings could be significantly reduced if nano/ultrafine grains were used at the bearing surface. The drive toward the use of ultrafine-grained materials and nanomaterials results mainly from the improvements in mechanical and wear properties they can offer [4–9]. The mechanical properties of nanoceramics such as hardness, strength and toughness are generally superior to those of conventional ceramics [10]. It is well known that the wear characteristics of conventional ceramics can be improved by reducing grain size [11, 12], and even more so by the use of nanoceramics [13]. In fact, the wear resistance of nano-composite alumina is up to two orders of magnitude superior to that of conventional alumina [13]. For these reasons, the study of ultrafine/nano-grained ceramic materials for bearing application is of high relevance and significant importance to a number of industries in addition to the biomedical (e.g. the cutting tool industry). One of the main impediments to the sintering of nanopowders to high density has been grain growth, resulting in the loss of the nanostructure. Another major drawback in the application of nano-materials is the general higher cost of the precursor nano-

*Author to whom all correspondence should be addressed

powders used compared to conventional ceramic powders. Functionally gradient materials (FGMs) are materials where the composition gradually or step-wise changes from the bulk to the surface [14], with the aim of gradually changing the material properties from bulk to the surface. FGMs have been produced in the past by a variety of processes including chemical vapor deposition (CVD), plasma spraying, hot pressing [15] and powder stacking methods. Although the CVD and plasma spraying processes can generate layers of controlled thickness, they are, however, expensive production routes compared to conventional process such as slip casting. In fact, sequential slip casting has been used successfully to produce functionally gradient materials where composite layers of different reinforcement volume fractions are deposited on one another [16–18]. Ceramic hip joint materials can normally be formed through the production of a green compact which is then subsequently sintered/hot isostatically pressed [19]. Alumina (Al_2O_3) is one of the most studied bioceramics due to its combined inertness and good mechanical properties [20–22], and was therefore used as our model material. Our aim is to apply sequential slip casting to the production of highly dense functionally gradient materials with respect to ''grain-size'' i.e. with a transition in grain size from one side of the material to the other. In the current work a simple disc geometry model is used in order to study the sintering behavior, with the view of extending our work to actual orthopedic parts. This paper reports the effect of hot pressing and pressure-less sintering on the microstructure of the final grain-size functionally gradient materials (GS-FGMs). Future strategies for achieving nanostructure at the surface are also identified.

Experimental procedure

Predominantly α-alumina powders (99.99% purity) (Baikowski International Inc., Charlotte, NC) of sizes 50, 100, 150 and 250 nm were used in our experiments to prepare separate aqueous slips. The solid volume fractions for each slip were 20 vol % for 50, 100 and 150 nm and 30 vol % for 250 nm particles with the balance being distilled water. An ammonium polyacrylate dispersant (Duramax™ D-3005, Rohm and Hass, PA) was added to each slip to enable good dispersion and de-agglomeration of the powders (indicated by a minimum in the apparent viscosity measured using a Brookfield viscometer) then ball milled for a period of 24 h. All slips were then degassed in a vacuum desiccator for 10–15 min to remove entrapped air bubbles left in the ceramic slips after ball milling. These slips were then sequentially slip cast in one inch (25.4 mm) internal diameter short cylinders placed on a plaster of paris base to form a functionally gradient ceramic green compact with layers of varying particle sizes along the height. The quantity of slip poured in each layer was pre-calculated to obtain final layers each approximately 1 mm thick assuming full densification after high temperature consolidation. The resulting green layered compact was then heated in an oven in air at a temperature of 60 °C for a period of 24 h to remove the residual moisture left in the green compact. Both pressure-less sintering and hot pressing were examined. Sintering was conducted at 1350 °C for 2 h with heating rate 20 °C/min to 850 °C and 1 °C/min to the sintering temperature. Hot pressing was conducted in a graphite die at 1350 °C for 30 min and 1400 °C for 30 min. In both hot pressing cycles, an initial pressure of 8 MPa was maintained during heating. The heating rate was 5 °C/min from room temperature to 750 °C, then the compact was heated at 30 °C/min to the hot pressing temperature where the pressure was increased to 30 MPa and maintained for 30 min. The pressure was then released and specimens left to cool in the die to room temperature. Green densities were measured by weighing the green compacts and dividing by their volume (measured using a micrometer and calipers). Final densities of the sintered/hot pressed compacts were measured using the Archimedes principle. Throughout the paper, all the layers will be referred to by their initial particle sizes, i.e. 50 nm original particle size layer (layer A), 100 nm original particle size layer (layer B), 150 nm original particle size layer (layer C) and 250 nm original particle size layer (layer D). All sintered/hot pressed specimens were sectioned centrally along the hot pressing direction in such a way as to expose the four layers of the cross-section for polishing operations and microstructural observations. Specimens were then ground and subsequently polished to a 15 μm, 6 μm, 1 μm and 50 nm diamond finish, each for a duration of 1 h. Micrographs of the polished and etched microstructures were taken using a field emission electron microscope. The area fraction of porosity in the central region within each layer was measured using a Buehler image analysis software, five areas were analyzed for each layer and a standard deviation calculated. Grain boundaries were revealed by thermal etching at a temperature 100 °C lower than the sintering/hot pressing temperature for 30 min. Grain size was measured using the linear intercept method and multiplying by 1.56. All Knoop microhardness measurements were conducted using a Buehler microhardness tester using an indentation load of 500 g.

Results and discussions

Pressure-less sintering

Fig. 1 shows a sequentially slip cast four-layer (50/100/150/250 nm) green compact. The optimized four-layer green compacts were first pressure-less sintered at

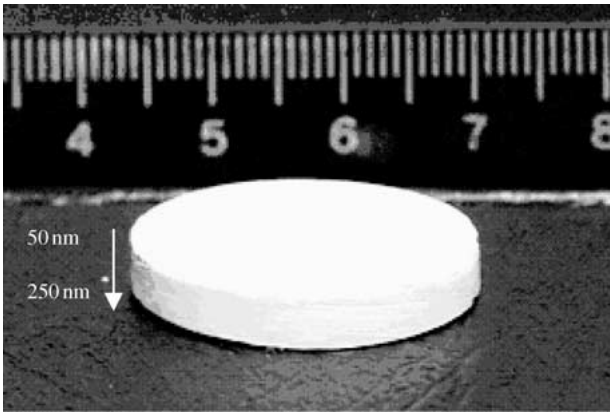

Figure 1 Four-layer (50/100/150/250 nm) functionally gradient ceramic slip cast specimen in the green state.

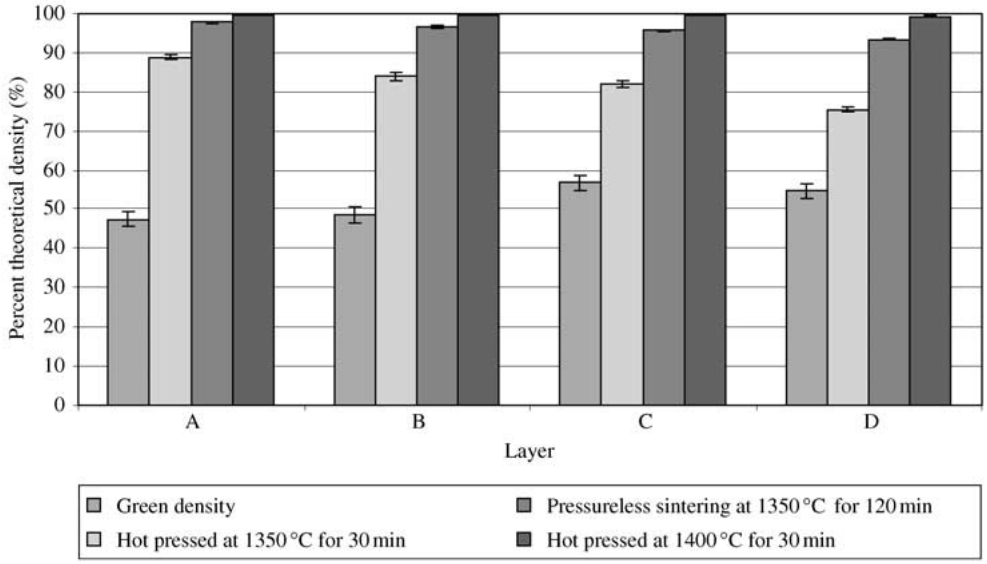

Figure 2 Percent theoretical density for layers A–D, green, pressure less sintered at 1350 °C for 120 min, hot pressed at 1350 °C for 30 min and hot pressed at 1400 °C for 30 min.

1350 °C for 2 h. On removal from the furnace, the sintered compact appeared intact, however, it appeared slightly tapered from layer D to layer A, with layer A having the smaller diameter. The green density of the layered compact was $54.1 \pm 0.8\%$ of theoretical compared to a sintered density of 79.5% of theoretical (3.98 g/cm^3 as quoted by the manufacturer). It was clear that sintering promoted densification; however, the individual layers were densified to different degrees. Fig. 2 includes data on the green and final densities for each layer. The percent theoretical density for each layer was found by measuring area fraction of porosity within each polished and un-etched layer. It can be seen from Fig. 2 that layer A exhibited the highest density of the four layers. This increased densification can be attributed to both a well-dispersed slip and a much higher particle surface area leading to a substantially higher driving force for sintering than the remaining layers. The particle surface area is decreased from layer A to D leading to a decrease in the driving force for sintering resulting in a corresponding decrease in the density. The overall low sintered density ($\sim 80\%$ of theoretical) of the layered compact raises doubt as to the suitability of pressure-less sintering as a viable processing route for this class of materials. Higher temperatures which should increase the density, however, will be at the expense of considerable grain growth. Sintering under an applied pressure (hot pressing) is seen as a more viable processing route.

On examination of the interfaces between different layers it was also observed that poor bonding existed in a number of regions along the interface line for all the layers, an example of which is shown in Fig. 3 for the interface between layers C and D. This is believed to be due to the inherent difference in shrinkage rates of the individual layers due to their different particle sizes and therefore driving force for sintering, which in turn caused the poor bonding. These poorly bonded areas resulted in a higher average density when measured using image analysis than that measured using the Archimedes method, since the former does not take into account poor interface bonding.

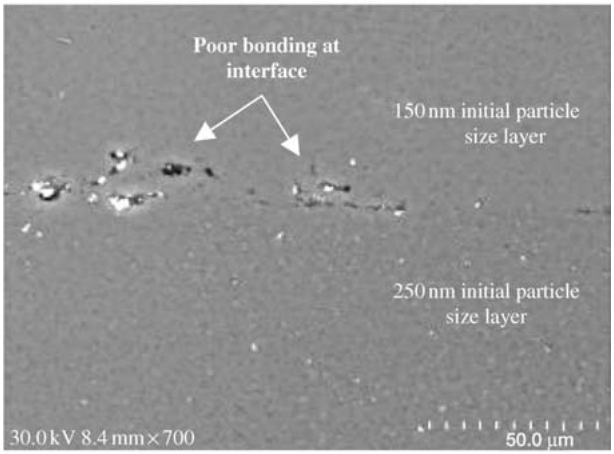

Figure 3 Electron micrograph showing poor bonding at interface between layers C and D for pressure-less sintered compact.

Hot pressing

The previous section demonstrated the inherent problems associates with pressure-less sintering which includes low density of the final product and poor bonding of layers. Hot pressing has the advantage of achieving better consolidation by increasing the particle contact stresses during sintering. When hot pressing was conducted at 1350 °C for 30 min, the resulting compact was found to have a bulk density of 95.6% with all layers perfectly bonded. Fig. 4 compares the thermally etched microstructures taken from the central region within each layer for of the 1350 °C hot pressed and pressure-less sintered specimens. It can be seen that in general, the hot pressed material has a higher density and smaller average grain size. The grain growth observed for the pressure-less sintered specimen is a direct result of the prolonged sintering time having been sintered for 90 min more than the hot pressed counterpart.

A bulk density of 95.6% will, however, unlikely yield the optimum mechanical properties needed in hip joint applications where products closer to full density would be more desirable. An increase in the hot pressing temperature by 50 °C from 1350 to 1400 °C resulted in an almost fully dense (99.8%) final compact. The percent

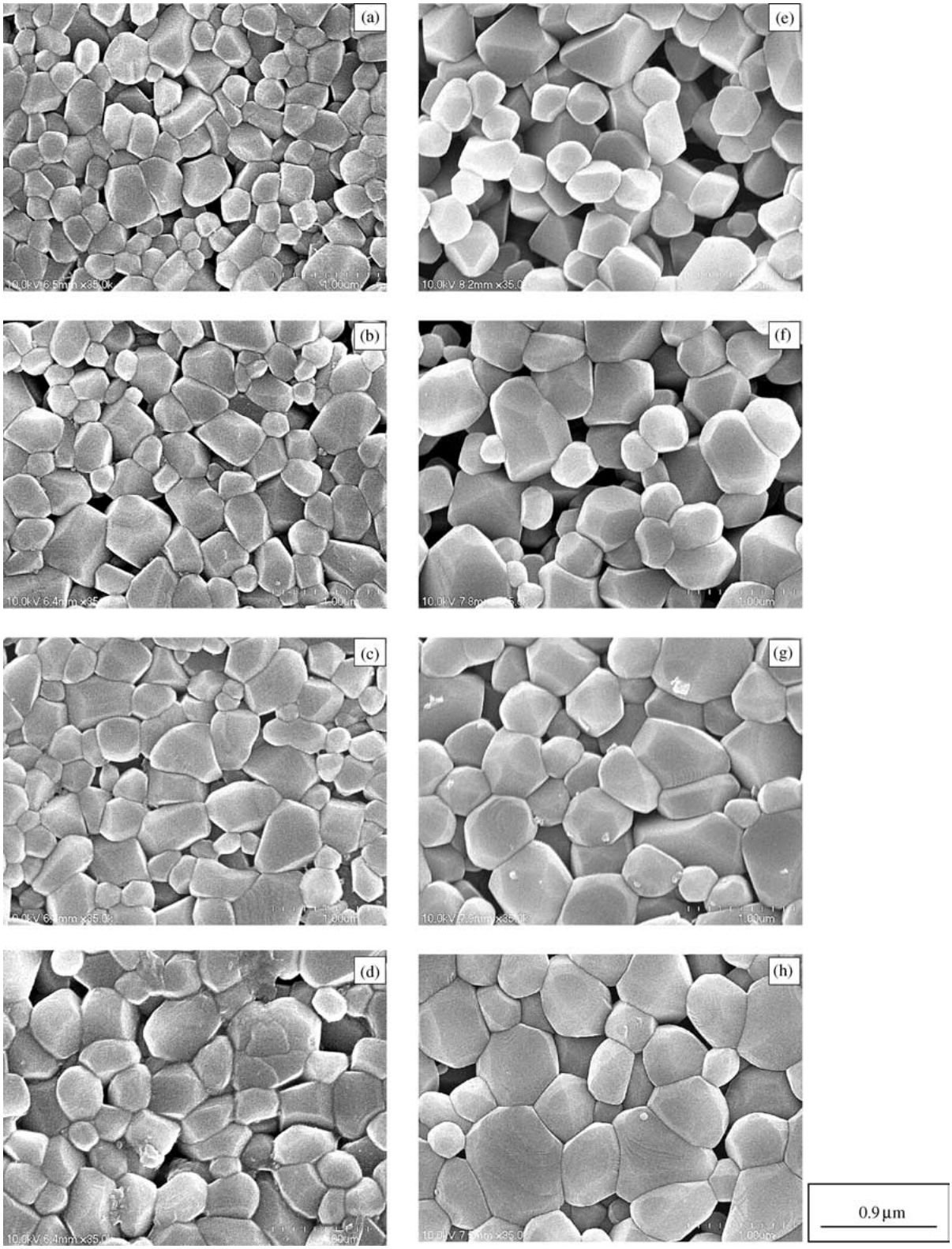

Figure 4 Electron micrographs of polished and thermally etched microstructure for layers A–D after hot pressing (a–d respectively) and pressure-less sintering (e–h respectively) at 1350 °C.

theoretical density of each layer for all the processed materials is presented in Fig. 2. It can be seen that hot pressing was essential in achieving high densities which is highest at 1400 °C (30 min). The micrographs in Fig. 5 clearly demonstrates that highly dense materials with a final grain size that increases from the surface inward have been successfully produced by hot pressing at 1400 °C for 30 min.

The average grain size in the surface layer was measured to be 382 $\pm$ 98 nm. It is believed that this grain size can be reduced to below 100 nm by increasing the pressure during hot pressing which would result in a reduction in the required hot pressing temperature, [23] and also the addition of grain growth inhibitors. The grain sizes of all layers for all the processed materials are summarized in Table I. It can be seen that hot pressing at 1400 °C for 30 min achieved a similar grain size in each layer to that pressure-less sintered at 1350 °C for 120 min

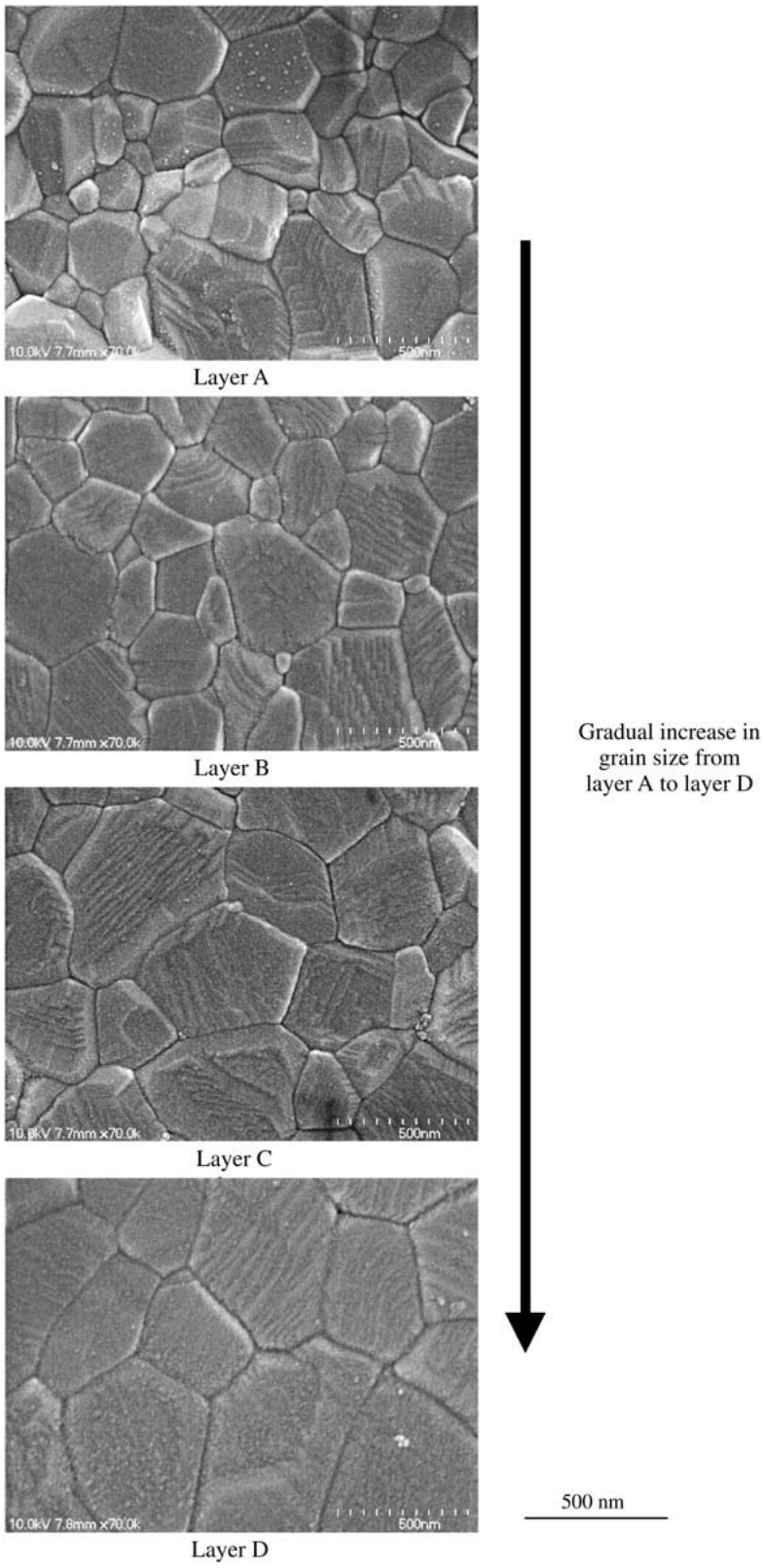

Figure 5 Grain-size functionally gradient alumina ceramic produced by hot pressing at 1400 °C for 30 min.

while at the same time achieving near full density. Hot pressing at 1350 °C gave the best results in terms of grain size; however, the bulk density of this specimen was only 95.6% of theoretical. It is well known that the grain growth rate is inversely proportional to grain size [24]. Accordingly, it is expected that after sintering or hot pressing, the finer the original particle size the larger the relative grain growth experienced. This was observed for all our processed materials where the ratio of the final grain size after hot pressing or pressure-less sintering to the original particle size is greatest for the 50 nm layers (layer A) and least for the 250 nm layers (layer D).

The differences in grain size from one side to the other can result in differences in strength and hardness (the smaller the grain size the higher the strength and hardness according to the Hall–Petch equation). Microhardness measurements were therefore conducted to probe into the mechanical response of our near full density (i.e. 1400 °C hot pressed) processed material. It is well known that in general, wear resistance may increase

TABLE I Effect of pressureless sintering and hot pressing on the grain size of individual layers

Process	Temperature (°C)	Time (mins)	Final grain size in layer A (nm)	Final grain size in layer B (nm)	Final grain size in layer C (nm)	Final grain size in layer D (nm)
Pressureless sintering	1350	120	376 ± 51	451 ± 92	495 ± 59	599 ± 59
Hot pressing	1350	30	301 ± 56	338 ± 48	372 ± 74	429 ± 58
Hot pressing	1400	30	382 ± 98	463 ± 44	497 ± 97	577 ± 78

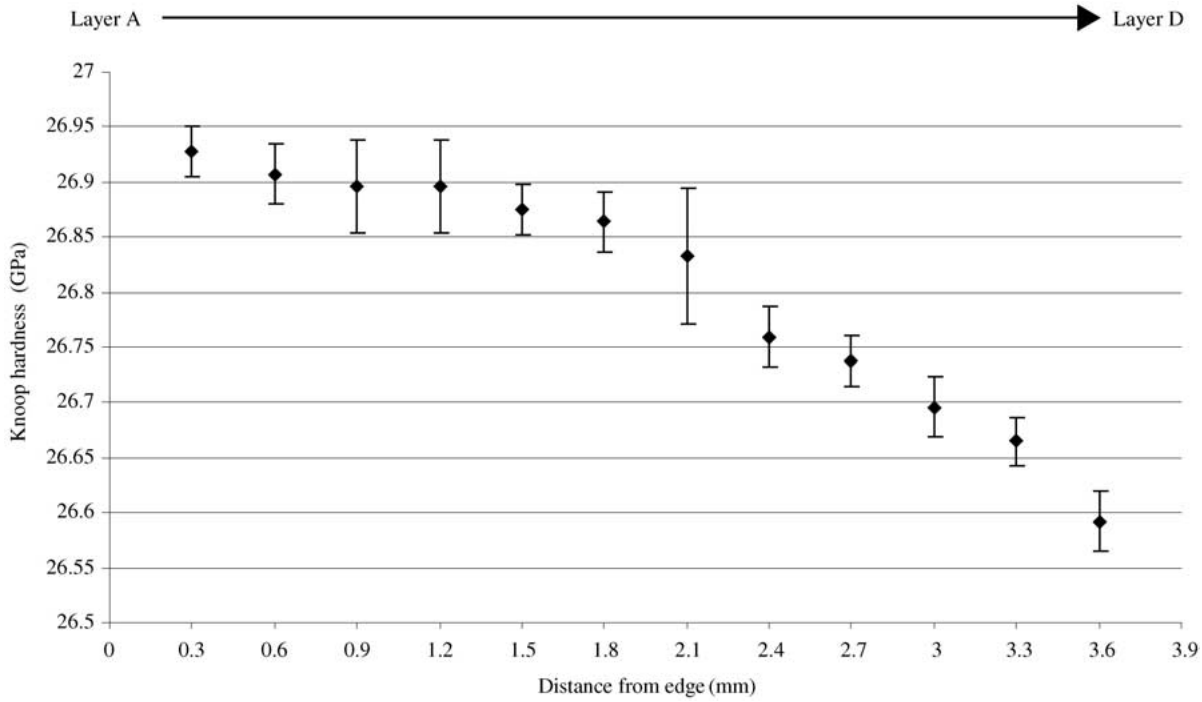

Figure 6 Micro-hardness as a function of distance beneath the surface of the 1400 °C hot pressed disc, showing a smooth transition in the hardness from surface to bulk layer (i.e. layers A–D, each layer ∼ 1 mm).

with increase in hardness [25, 26] (although other properties including fracture toughness and Young's modulus need also to be considered). In the application of the final implant materials it is not only important that the surface hardness be maximized through smaller grain sizes (on the nano-scale) but that there should preferably be no abrupt change in properties from the surface inwards. Fig. 6 is a hardness profile taken from the cross-section of the polished hot pressed material. It is clear that the hardness changes gradually from one side of the specimen to the other. It must also be mentioned that some carbon may have diffused into the specimen through the contact with graphite which may have possibly influenced the hardness. Nevertheless, our material does exhibit a decrease in final average grain size from one side to the other which according to the Hall–Petch equation should exhibit a change in hardness. The maximum hardness of approximately 26.9 GPa was observed for the 50 nm original particle size layer (having a final grain size of 382 ± 98 nm, Table I). This is significantly higher than a reported value of ∼ 19 GPa for ∼ 2 μm grain size alumina [27] (a typical grain size of implanted alumina [28]). This may be reflected in an increase in wear resistance however; this needs to be verified through a detailed examination of wear properties of these materials (the subject of on-going work).

Conclusions

Experiments were conducted on the processing of bioceramics functionally graded with respect to grain size. The following conclusions can be drawn:

1. Pressure-less sintering was found unsuitable under the investigated processing conditions for producing functionally gradient ceramics with respect to grain size owing to poor densification and poor bonding at the interfaces between layers.
2. Hot pressing provided increased densification and good bonding at interfaces; density was highest for the 1400 °C hot pressed material.
3. The final grain size was successfully made to decrease gradually from one side of the sintered and hot pressed compacts to the other side, with a hardness profile exhibiting a gradual increase from one side of the specimen to the other.
4. The extent of grain growth was found to decrease from the finer to the coarser particle size layers for all our processed materials.
5. The results may provide important implications for the production of grain-size functionally gradient orthopedic implants with superior wear resistance. This will be investigated and confirmed through characterization of mechanical and wear properties of optimized materials (the subject of on-going work).

Acknowledgments

The authors would like to thank the Missouri Foundation for Medical Research for their much appreciated support in the initiation of this work through grant no. 041801.

References

1. D. A. PULEO and A. NANCI, *Biomaterials* **20** (1999) 2311.
2. S. B. BAL, D. VANDELUNE, D. M. GURBA and W. H. HARRIS, *J. Arthroplasty* **13** (1998) 492.
3. E. J. HENSSGE, I. BOS, G. WILLMANN, *J. Mater. Sci.-Mater. Med.* **5** (1994) 657.
4. C. SURYANARAYANA, *J.O.M.* **54** (2002) 24.
5. W. L. GAO et al., *J. Inorg. Mater.* **15** (2000) 1005.
6. M. MITOMO, YOUNG-WOOK KIM and H. HIROTSURU, *J. Mater. Res.* **11** (1996) 1601.
7. X. H. JIN, L. GAO, L. H. GUI and J. K. GUO, *ibid.* **17** (2002) 1024.
8. HAE-WON KIM, YOUNG-HAG KOH and HYOUN-EE KIM, *ibid.* **15** (2000) 1478.
9. A. S. EDELSTEIN and R. C. CAMMARATA, in ''Nanomaterials: Synthesis, Properties and applications'' (Institute of Physics Publishing, London, 1998) p. 332.
10. A. S. EDELSTEIN and R. C. CAMMARATA, in ''Nanomaterials: Synthesis, Properties and applications'' (Institute of Physics Publishing, London, 1998) p. 188.
11. C. P. DOGAN and J. A. HAWK, *Wear* **225** (1999) 1050.
12. A. KRELL and D. KLAFFKE, *J. Am. Ceram. Soc.* **79** (1996) 1139.
13. J. RODRIGUEZ, *ibid.* **82** (1999), 2252–2254.
14. Y. MIYAMOTO, W. A. KAYSSER, B. H. RABIN, A. KAWASAKI and R. G. FORD, in ''Functionally Graded Materials: Design, Processing and Applications'' (Kluwer Academic Publishers, Boston,1999) p. 1.
15. A. KAWASAKI and R. WATANABE, in ''Ceramics: Charting the future: Advances In Science and Technology'', Proceedings of the 8th CIMTEC-World Ceramics Congress and Forum on New Materials, Florence, Italy, 28 June 1994, p. 1715.
16. J. S. MOYA, A. J. SANCHEZ-HERENCIA, J. REQUENA and R. MORENO, *Mater. Lett.* **14** (1992) 333.
17. I. M. G. DOS SANTOS, R. C. M. MOREIRA, E. R. LEITE, E. LONGO and K. A. VARELA, *Ceram. Int.* **27** (2001) 283.
18. H. TAKEBE and K. MORINAGA, *Mater. Manuf. Proc.* **9** (1994) 721.
19. I. STAMENKOVIC and A. SALOMONI, *Ceram. Acta* **10** (1998) 11.
20. K. MORSI, ''Mechanical Properties of Particle Reinforced Alumina'' (Ph.D. Thesis, University of Oxford, UK, 1996).
21. R. I. TODD, K. MORSI and B. DERBY, *Br. Ceram. Proc.* **57** (1997) 87.
22. K. MORSI and B. DERBY, *Br. Ceram. Trans.* **98** (1999) 72.
23. R. S. MISHRA, E. L. CHARLES and K. M. AMIYA, *J. Am. Ceram. Soc.* **79** (1996) 2989.
24. W. D. KINGERY, H. K. BOWEN and D. R. UHLMANN, in ''Introduction to Ceramics'', 2nd edn. (Wiley Interscience New York, 1976) p. 454.
25. K. H. W. SEAH, R. S. KULKURNI, S. C. SHARMA and A. RAMACHANDRA, *J. Mater. Sci. Tech.* **12** (1996) 357.
26. C. J. OH, S. LEE and M. G. GOLKOUSKI, *Met. Mater. Trans. A* **32** (2001) 2995.
27. S. D. SKROVANEK and R. C. BRADT, *J. Am. Ceram. Soc.* **62** (1979) 215.
28. J. L. KATZ, Orthopedic applications, in ''Biomaterials Science—An Introduction to Materials in Medicine'', edited by B. D. Ratner, A. S. Hoffman, F. J. Schoen and J. E. Lemons, (Academic Press, California, 1996) p. 343.

Received 31 December 2002
and accepted 3 April 2003